

## Spray Combustion Characteristics of Octanal and Diesel

Irene Ruiz-Rodriguez\*<sup>1</sup>, Thanos Megaritis<sup>1</sup>, Lionel Ganippa<sup>1</sup>

<sup>1</sup>Mechanical, Aerospace and Civil Engineering Department, Brunel University London, UB8 3PH

\*Corresponding author: [irene.ruizrodriguez@brunel.ac.uk](mailto:irene.ruizrodriguez@brunel.ac.uk)

### Abstract

Soot particles are noxious emissions that are associated with global warming and are known to be harmful to humans. They are partly produced from the combustion of hydrocarbon fuels, and can be reduced by altering the fuel structure. For this, adding an oxygen moiety becomes an attractive solution to simultaneously reduce the soot formation and to enhance its oxidation. Nonetheless, the oxygenated fuel must meet several criteria to be a candidate to replace or to blend with diesel in the current engine infrastructure. For example, it must have similar physical properties and a similar energy content to diesel. One of the promising fuels that could meet these criteria is octanal. However, data on its spraying and combustion characteristics are not known, and neither fundamental studies nor studies under engine-like conditions are available in the literature to characterise the spray combustion of octanal.

To fully characterise the potential of an oxygenated fuel and its sooting propensity, both its spray and spray combustion characteristics must be understood. In this work, the latter is addressed to build up on the knowledge about this fuel and gauge its potential as a possible blend or as an alternative to diesel. In order to explore the combustion properties of octanal, we evaluated the soot and temperature distribution by using a two-colour pyrometry system coupled with a high-speed camera. The same mass of diesel and octanal was injected into an engine-like, high temperature, high pressure environment, using a multi-hole common rail injector. This allowed for a relative comparison of the combustion of each fuel spray. It was discovered that the sooting characteristics of diesel and octanal were fundamentally different, owing to the difference in thermochemical properties. For a similar flame temperature, it was observed that octanal produced less soot than diesel.

### Keywords

Spray combustion, oxygenated fuels, octanal, high pressure chamber, two-colour pyrometry

### Introduction

The use of diesel engines is still widespread in the transportation industry, and they are needed especially in the heavy-duty sector to power vehicles carrying heavy loads. It is therefore important to continue optimising them and developing strategies to reduce the emissions. Of concern for the sector are both the depletion of fossil fuels and the emission of noxious combustion products, such as soot. Due to the current climate regarding internal combustion engines, targeting an improvement in these areas from a spray and combustion point of view becomes important, and one such way of doing so is finding suitable replacements for diesel that can be blended with it or directly replace it. Oxygenated fuels are sound candidates for this, as due to the in-bound oxygen the soot formation rate can be reduced and the oxidation enhanced [1,2]. Whilst the spray and combustion characteristics of several different alcohols, esters and some ketones have been reported in the literature [3–7], fundamental optical spray combustion studies are lacking for oxygenated fuels which have high carbon numbers and which would match better diesel's thermo-chemical properties.

One such fuel that *a priori* could be a suitable candidate is octanal. It is an aldehyde with eight carbons, a chemical formula of  $C_8H_{16}O$  and a chemical structure as shown in Figure 1. Its density is  $821 \text{ kg/m}^3$  and its lower calorific value (LCV) is almost  $40 \text{ MJ/kg}$ , properties that resemble those for diesel ( $\sim 850 \text{ kg/m}^3$  and  $\sim 43 \text{ MJ/kg}$ ).

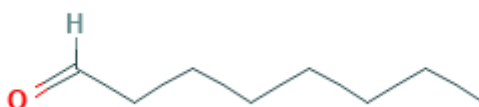


Figure 1. Octanal's chemical structure

In this work, the spray combustion characteristics of octanal and diesel were studied and compared by using the two-colour pyrometry system coupled with high-speed imaging. The resulting soot and temperature distribution across different portions of the flame were analysed to determine any differences in the development of the

combustion process. These preliminary results show that octanal could be an attractive candidate for use in diesel engines to aid on the reduction of soot emissions.

### The constant volume chamber

The neat fuels were injected into a constant volume chamber (CVC) at controlled ambient conditions with a temperature of around 1300K to reduce the effects of pre-mixing. The same amount of fuel mass was used for both, and the fuel was injected at 700bar using a six-hole common rail diesel injector to study the fundamentals of spray combustion. To maximise the resolution of the data, only one of the six spray flames was imaged for 10 combustion events for each fuel. The same flame was imaged twice by using the combination of a beam splitter and a mirror, and each image was passed through a different narrow band-pass filter (green and red) to obtain the soot radiation at two wavelengths, required for the use of the two-colour pyrometry method as discussed in the next section. A schematic of the set-up used to collect the data is presented in Figure 2.

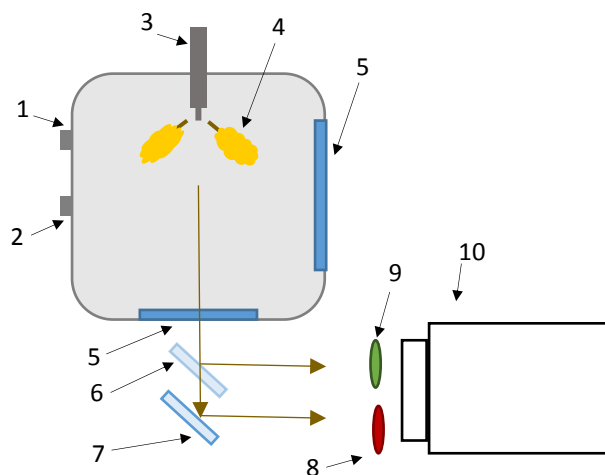


**Figure 2.** Experimental set-up of the CVC and the two-colour pyrometry system used to collect the data: 1. Exhaust; 2. Inlet; 3. Injector; 4. Sample flame; 5. Optical access; 6. Beam splitter; 7. Mirror; 8. Red narrow band-pass filter; 9. Green narrow band-pass filter; 10. High-speed camera

### Two-colour pyrometry

The two-colour pyrometry method is versatile, has been widely used in the literature and allows for a non-intrusive way of collecting both soot and temperature data simultaneously [8–10]. It is important to note that errors can be induced from the system calibration, collection optics, camera discretization levels and other method-induced ones, which make the two-colour method semi-qualitative in nature. Two-colour pyrometry results are based on line-of-sight measurements, which can result in a reduction of apparent signal intensity due to self-absorption effects in optically thick regions of the flame- in particular for diesel flames. Due to space limitations, these errors are not discussed in detail in this paper but a discussion of them can be found in [11–13]. A brief outline of how the method works is provided below.

The two-colour method makes use of the dependence of radiation on wavelength and temperature, whereby the soot radiance ( $I_S$ ) is a multiple of the black-body radiance ( $I_B$ ) at the same temperature ( $T$ ) and wavelength ( $\lambda$ )- with the emissivity of soot ( $\epsilon$ ) taking a value of less than one for a non-blackbody emitter. Following Planck's law, the blackbody radiation can be expressed in terms of two constants ( $c_1$  and  $c_2$ ),  $T$  and  $\lambda$ . This can be seen in equation (1). The emissivity can be expressed using a semi-empirical relation as discussed in [14] and as shown in equation (2), and is dependent on: the dispersion exponent ( $\alpha$ ) that takes a value of 1.39 in the visible wavelength range [13];  $KL$ , which is the soot optical thickness; and  $\lambda$ . It has been shown in previous works that the dispersion exponent can be considered to be fixed for most fuels when working in the visible wavelength range [14,15]. The radiance that is captured by the sensor, which in this case is a high-speed camera, is normally available in arbitrary units. To obtain radiance units and be able to use equations (1) and (2), a calibration procedure with a light source of a known radiance was performed to obtain the camera intensity in terms of radiance.

$$I_S = \epsilon I_B \rightarrow \epsilon \frac{c_1}{\lambda^5 [\exp(\frac{c_2}{\lambda T}) - 1]} \quad (1)$$

$$\varepsilon = 1 - \exp\left(-\frac{KL}{\lambda^{\alpha}}\right) \quad (2)$$

By solving these equations at two different wavelengths,  $\lambda_1$  and  $\lambda_2$ , (filtered using narrow band-pass filters with wavelengths centred at values of 543.5nm and 670nm to avoid the interferences of bands of flame radicals) the temperature and KL factor values were obtained at every pixel location. This was done using the local radiance values obtained for every flame pixel in the images. Once the temperature and KL factor values were obtained for every injection event, these were averaged to obtain mean representative values of both parameters at every point in time.

## Results and discussions

This section is divided into two subsections: the first one discusses the temperature distributions across the flame and the second one discusses the soot distribution across the flame. It is noted that in this work, octanal was injected neat into the CVC using a standard common rail fuelling system, and some qualitative observations were made regarding its compatibility with the system. Firstly, even though some premature aging of the injector tip was observed (brown rust flakes covering the injector tip), no significant alteration of the injection behaviour was observed as the injection duration remained the same and no injection failures were recorded. Secondly, no change in operational behaviour or damage was observed in the pumping system that we used. These preliminary observations show that octanal is potentially compatible with current injection hardware. Nonetheless, more quantitative data are needed to support these observations.

### Temperature distribution across the flame

The temperature distribution across the flame is presented in Figure 3 and the images corresponding to the points in time presented are shown in Figure 4. The data in Figure 3 were obtained by firstly, drawing a line from the start of the flame, passing through its centre and ending at the tip of the flame. At around 8 locations along this centre-line, perpendicular lines were drawn to cover the width of the flame. The values for the temperature across these perpendicular lines were then averaged to obtain one value for the temperature at that point on the flame for the 8 locations studied. A sample of this concept is shown in Figure 5.

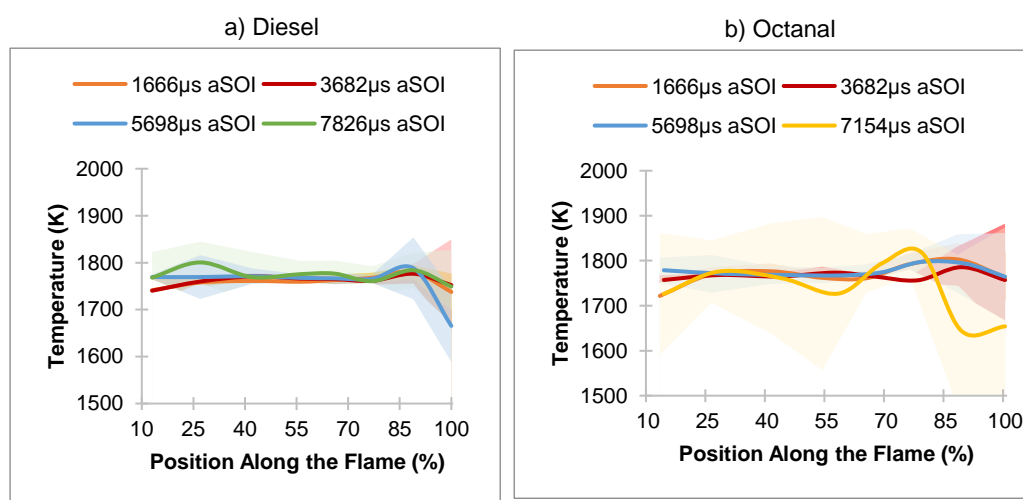


**Figure 3.** Averaged temperature distribution (of 10 combustion) events at different point in times- 0% is the start of the flame and 100% the tip of the flame a) diesel and b) octanal. Error bands represent two standard deviations

It was found that the combustion of the octanal spray was faster than for diesel, as the end of combustion (EoC) was observed to be around  $\sim 7000\mu\text{s}$  after the start of injection (aSOI) for octanal and  $\sim 8800\mu\text{s}$  aSOI for diesel. This earlier EoC for octanal was caused by its fuel-bound oxygen content, which enhanced the oxidation of soot towards the EoC. For both fuels, it seems that overall, the average temperature across the flame remained fairly constant throughout the first three selected times aSOI up to the point where the end tip of the flame was reached. At the end point, a small temperature increase was observed, due to the larger amount of fresher oxygen available for combustion at the flame tip. It is also noted that there were no large differences in the average temperature values for both fuels, which could be partly attributed to the similar calorific value of 43MJ/kg and 40MJ/kg for diesel and octanal respectively. As combustion approached the final stages ( $>7826\mu\text{s}$  aSOI for diesel and  $>7154\mu\text{s}$  aSOI for octanal), for diesel, the high temperature regions accumulated at the tip whereas for octanal the temperature

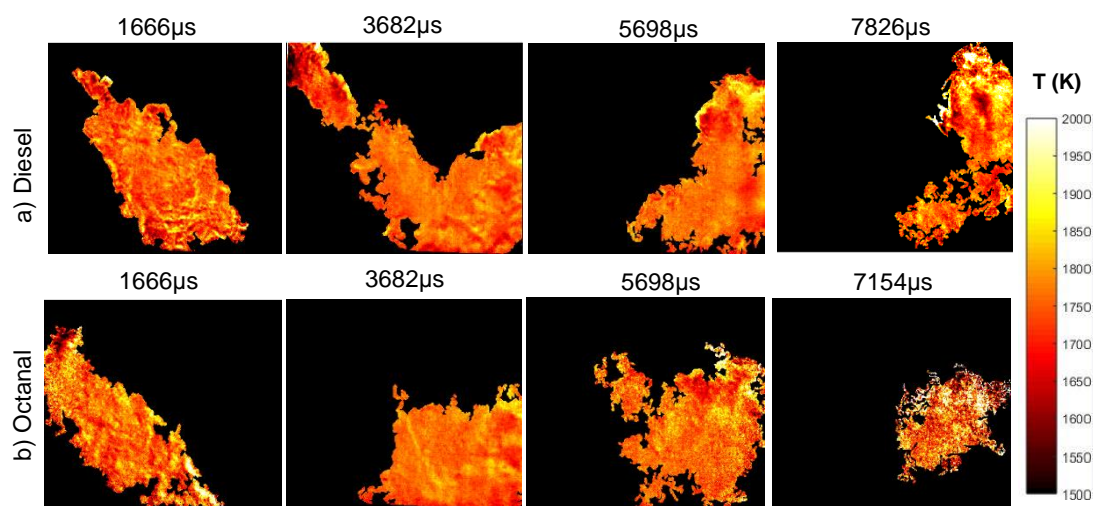


**Figure 4.** Two-colour pyrometry images for the points in time presented in Figure 3. The images are for a single combustion event. Set a) for diesel and set b) for octanal

distribution became somewhat variant. For diesel, these high temperature regions were caused by the oxidation of the final pockets of soot in a region where more oxygen was available for it. For octanal, both high and low temperature patches were randomly distributed across the flame, causing the average temperature to increase and decrease throughout. This could be a result of the fuel-bound oxygen content of octanal, which gives soot more chances to oxidise at different locations inside the flame.

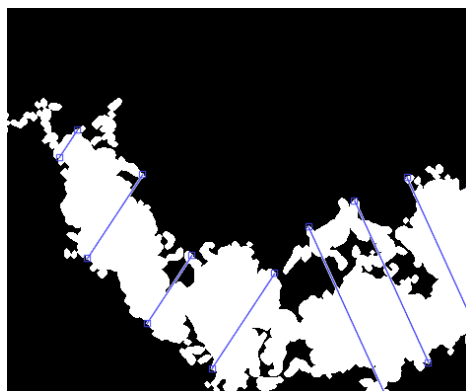


**Figure 5.** Sample of how the partitions were done to obtain the data presented in the graphs

### Soot distribution across the flame

The data presented in Figure 6 were obtained in a similar manner to those in Figure 3, as described in the previous section. However, in this case, the graphs represent the sooting tendencies of each fuel as a function of the KL factor. Figure 6 shows the two-colour results for the KL factor spatial distribution and Figure 7 the images for those points in time. From Figure 6 and Figure 7, it becomes apparent that at every point in time, diesel soots more than octanal, and that for diesel, the high sooting values are present in more parts of the flame. On average, the maximum KL factor attained for diesel is 2.2 and for octanal this maximum is 1.7, which constitutes a reduction of 23% in average peak soot for the points studied across the flame. Several factors could be causing the observed results, for example, the smaller carbon chain of octanal when compared to diesel or the effect of the oxygen moiety in octanal hindering soot formation and promoting soot oxidation. Some differences in soot distribution across the flame also exist between both fuels, especially during the middle combustion stages.

For the start of combustion (SOC) ( $\sim 1666\mu\text{s}$  aSOI) and the EOC ( $>7826\mu\text{s}$  aSOI for diesel and  $>7154\mu\text{s}$  aSOI for octanal), it can be seen that the distribution is similar but with different quantitative values. During the SOC most of the soot distributes towards the middle and tip of the flame and towards the EOC, most of the soot has oxidised and only a small amount remains at the flame tip. During the middle stages of combustion, at around  $3682\mu\text{s}$  aSOI, soot appears in several portions of the flame for diesel whereas for octanal the higher sooting regions accumulate at the tip only and have a lower value when compared to diesel at the same time aSOI. These results show that octanal hinders the formation of soot precursors when compared to diesel and delays the onset of significant sooting regions to the tip of the flame. When looking at the later middle stages of combustion ( $>5698\mu\text{s}$  aSOI), for octanal there is a more abrupt decrease in the amount of soot than for diesel, for which the decrease is more gradual and high sooting regions persist towards the middle and end of the flame. This indicates that octanal enhances the oxidation of the soot when compared to diesel.

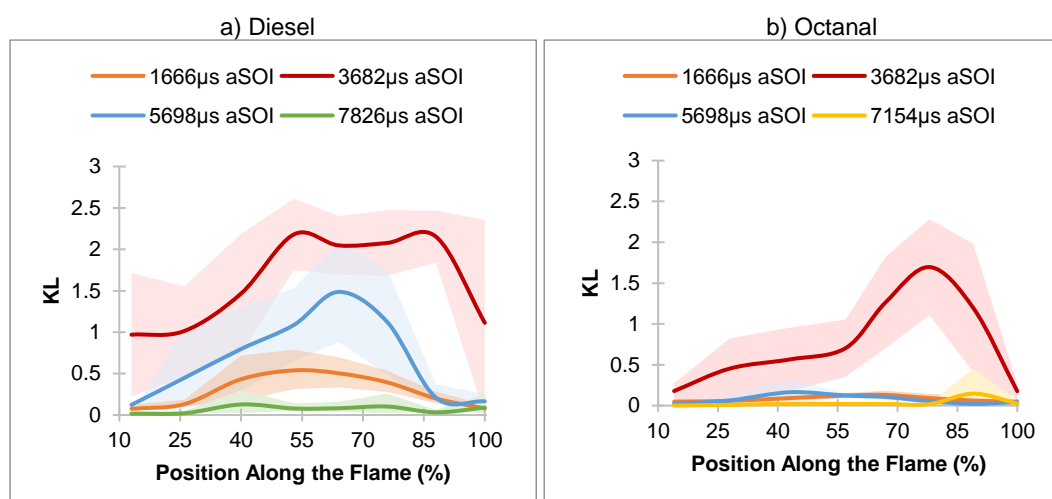


**Figure 6.** Averaged KL distribution (of 10 combustion events) at different point in times- 0% is the start of the flame and 100% the tip of the flame a) diesel and b) octanal. Error bands represent two standard deviations

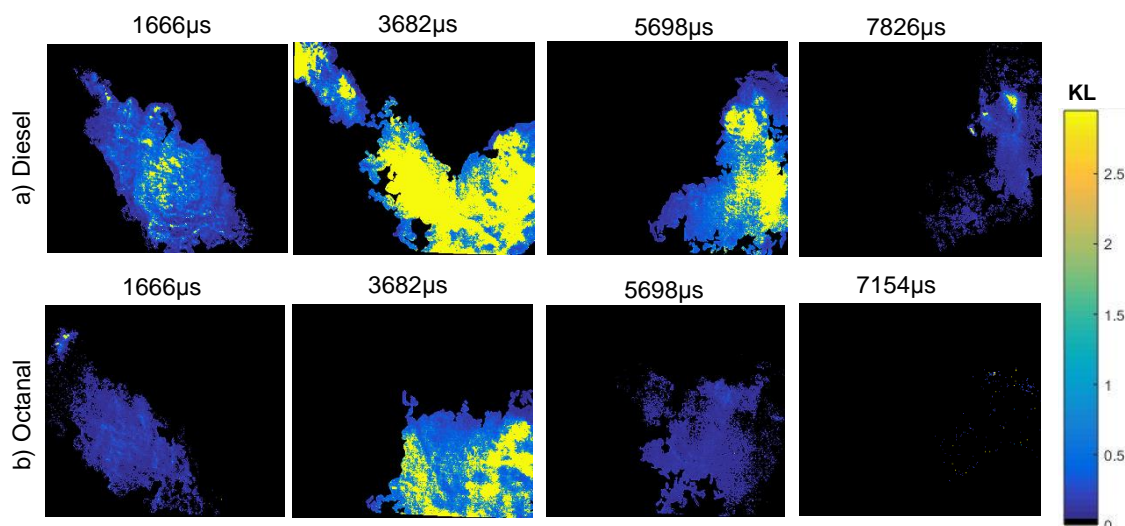


**Figure 7.** Two-colour pyrometry images for the points in time presented in Figure 6. The images are for a single combustion event. Set a) for diesel and set b) for octanal

## Conclusions

In this work, the spray combustion of octanal was studied and compared to diesel using a two-colour pyrometry system coupled with a high-speed camera. The emphasis was on studying the temperature and soot distribution across different parts of the flame. For most parts of the combustion period, both diesel and octanal had a similar temperature distribution across the flame until the end of combustion was reached. At this point, towards the tip of the flame, octanal exhibited more regions with higher and lower temperatures. Regarding the soot distribution, the first finding was the substantial reduction of soot when fuelling with octanal. Contrary to the temperature

distributions, the soot distributions between fuels did exhibit some differences. The soot produced by diesel was higher at earlier points in time with a tendency to accumulate towards the tip and middle parts of the flame. The soot produced by octanal tends to accumulate at the tip only and then rapidly oxidise towards the later combustion stages much faster than for diesel.

### Acknowledgements

This work was financially supported by the EPSRC.

### Nomenclature

|            |   |
|------------|---|
| $c_1$      | $1.1910439 \times 10^{-16}$ [ $\text{W m}^2 \text{sr}^{-1}$ ] |
| $c_2$      | $1.4388 \times 10^{-2}$ [mK]                                  |
| I          | radiance [ $\text{W/sr m}^2 \text{nm}$ ]                      |
| KL         | soot optical thickness  |
| LCV        | lower calorific value [MJ/kg]                                 |
| T          | temperature [K]   |
| $\alpha$   | dispersion exponent   |
| $\epsilon$ | emissivity  |
| $\lambda$  | wavelength [nm]   |

### References

- [1] Mueller, C. J., and Martin, G. C., 2002, "Effects of Oxygenated Compounds on Combustion and Soot Evolution in a DI Diesel Engine: Broadband Natural Luminosity Imaging," (724).
- [2] Iannuzzi, S. E., Barro, C., Boulouchos, K., and Burger, J., 2016, "Combustion Behavior and Soot Formation/Oxidation of Oxygenated Fuels in a Cylindrical Constant Volume Chamber," *Fuel*, **167**, pp. 49–59.
- [3] Heuser, B., Laible, T., Jakob, M., Kremer, F., and Pischinger, S., 2014, "C8-Oxygenates for Clean Diesel Combustion."
- [4] McEnally, C. S., and Pfefferte, L. D., 2011, "Sooting Tendencies of Oxygenated Hydrocarbons in Laboratory-Scale Flames," *Environ. Sci. Technol.*, **45**(6), pp. 2498–2503.
- [5] Deshmukh, D., and Ravikrishna, R. V., 2011, "Experimental Studies on High-Pressure Spray Structure of Biofuels," *At. Sprays*, **21**(6), pp. 467–481.
- [6] Shi, Q., Li, T., Zhang, X., Wang, B., and Zheng, M., 2016, "Measurement of Temperature and Soot (KL) Distributions in Spray Flames of Diesel-Butanol Blends by Two-Color Method Using High-Speed RGB Video Camera," *SAE Tech. Pap.*, **2016-Octob.**
- [7] Gonzalez, U., and Schifter, I., 2017, "Oxygenated Fuels Properties and Its Relationship with Engine Performance in Port Fuel Injection Engines.," (September), pp. 6–8.
- [8] Zhang, J., Jing, W., Roberts, W. L., and Fang, T., 2014, "Soot Measurements for Diesel and Biodiesel Spray Combustion under High Temperature Highly Diluted Ambient Conditions," *Fuel*, **135**(x), pp. 340–351.
- [9] Zhang, J., Jing, W., Roberts, W. L., and Fang, T., 2013, "Soot Temperature and KL Factor for Biodiesel and Diesel Spray Combustion in a Constant Volume Combustion Chamber," *Appl. Energy*, **107**, pp. 52–65.
- [10] Choi, C. Y., and Reitz, R. D., 1999, "Experimental Study on the Effects of Oxygenated Fuel Blends and Multiple Injection Strategies on DI Diesel Engine Emissions," *Fuel*, **78**(11), pp. 1303–1317.
- [11] Payri, F., Pastor, J. V., García, J. M., and Pastor, J. M., 2007, "Contribution to the Application of Two-Colour Imaging to Diesel Combustion," *Meas. Sci. Technol.*, **18**(8), pp. 2579–2598.
- [12] Di Stasio, S., and Massoli, P., 1994, "Influence of the Soot Property Uncertainties in Temperature and Volume-Fraction Measurements by Two-Colour Pyrometry," *Meas. Sci. Technol.*, **5**(12), pp. 1453–1465.
- [13] Ladommatos, N., and Zhao, H., 1994, "A Guide to Measurement of Flame Temperature and Soot Concentration in Diesel Engines Using the Two-Colour Method Part II: Implementation," *SAE Tech. Pap.* 941957, (941957).
- [14] Hottel, H. C., and Broughton, F. P., 1932, "Determination of True Temperature and Total Radiation from Luminous Gas Flames: Use of Special Two-Color Optical Pyrometer," *Ind. Eng. Chem. - Anal. Ed.*, **4**(2), pp. 166–175.
- [15] Zhao, H., and Ladommatos, N., 1998, "Optical Diagnostics for Soot and Temperature Measurements in Diesel Engines," *Prog. Energy Combust. Sci.*, **24**(97), pp. 221–255.